Proceedings World Geothermal Congress 2020+1
Reykjavik, Iceland, April - October 2021

Stress Field Evaluation with Application to Geomechanical Modeling of the Cement Sheath Integrity: A Case Study of the Los Humeros Geothermal Field, Mexico

[1]Michal Kruszewski, [2]Giordano Montegrossi, [3]Miguel Ramirez, [1]Volker Wittig, [3]Adrian Gomez Garcia, [3]Marcela Sanchez, and [1]Rolf Bracke

[1]International Geothermal Centre (GZB), Lennershofstraße 140, 44801, Bochum, Germany

[2]National Research Council of Italy (CNR), Via G. Moruzzi 1, 56124, Pisa, Italy

[3]Comisión Federal de Electricidad (CFE), Alejandro Volta 655, 58290, Morelia, Mexico

michal.kruszewski@hs-bochum.de

montegrossi@igg.cnr.it

marcela.sanchez@cfe.gob.mx

volker.wittig@hs-bochum.de

marcela.sanchez@cfe.gob.mx

rolf.bracke@hs-bochum.de

Keywords: in-situ stresses, cementing operations, wellbore integrity, high-temperature wells

ABSTRACT

This study presents a solid approach for computing the base data needed for the geomechanical modeling, using non-direct stress measurements such as circulation fluid losses, mechanical caliper log, and continuously measured drilling parameters. The in-situ stresses computed were fed to the analytical model for predicting the cement sheath integrity with the incorporation of wire-line acoustic measurements of the annular cement. The developed method, accounting for mechanical properties of a coupled casing-cement-rock system with the influence of temperature, internal wellbore pressures, and in-situ stresses, can be easily and without additional costs used to evaluate cement sheath integrity during various stages of a geothermal well lifecycle, and help to design drilling, production, and maintenance operations. The investigation carried out in this paper was based on the results from deep drilling operations in the Los Humeros Geothermal Field located at the border of Veracruz and Puebla states in Mexico, where downhole temperatures above the critical point of pure water were recorded, and hostile reservoir fluids were produced. Throughout almost 40 years of drilling operations in the field, issues related to wellbore stability and cement sheath integrity have been observed.

1. INTRODUCTION

While evaluating in-situ stress conditions in the reservoir it is often assumed that one of the principle stresses is vertical. Using this technique, vertical stress (S_v) can be calculated assuming the density of the overburden and the gravitational acceleration constant (Zoback 2007). The two other principal stresses are considered to be horizontal and are denoted as a minimum (S_{hmin}) and maximum (S_{Hmax}). Contrary to S_v, they are not so straightforward to determine, as they vary greatly with lithology, geothermal gradient, fluid flow, thermal anomalies and are controlled by the local and regional stresses. Having solid knowledge about the stress state of the reservoir, many issues such as wellbore stability and placement, fracture orientation and propagation or production-related subsidence can be addressed. One of the potentially most important aspects connecting reservoir in-situ stress conditions and long-term integrity of the wellbore is the annular cement sheath design.

The primary cementing operation is a crucial activity carried out during drilling of any type of deep geothermal well. Three of the main purposes of the primary cementing job are to assure zonal isolation, provide mechanical support for casing strings, and protect well construction against corrosion resulting from the often-hostile fluids, throughout the entire well life cycle including abandonment phase. When one of these points is not achieved, wellbore integrity is compromised. High-temperature geothermal wells proved to have an issue with providing mechanical support. Additionally, zonal isolation may not be a key requirement in such cases due to the extensive water circulation, common for the hydrothermal geothermal systems. Such phenomenon has been however changing as much deeper and hotter wells, frequently with multiple and separated aquifers with different fluid chemistry and temperatures, are being drilled, with the Los Humeros Geothermal Field (LHGF) being one of such examples (Kruszewski and Wittig, 2018).

The determination of adequate mechanical properties allows to characterize cement sheath stresses under reservoir conditions and to predict whether, how and at which depth annular cement might potentially fail. Wrongly selected parameters might lead to the loss of wellbore integrity, even at early stages of well's life cycle. Properly executed cementing operation provides a sound cement sheath of very low permeability, which excludes any potential fluid migration (Nelson and Guillot 2006). A badly executed cementing job might result in chimneys, channels or, at some extreme cases, loss of all pumped cement into the adjacent formations (Loizzo 2014). Fluid sections, entrapped between cemented casing strings or cemented casing and impermeable formations without a possible relief pathway, can expand during the fluid production phase or heating-up, compromising cement integrity and eventually leading to an undesirable event of casing collapse, as presented in Figure 1 on an example from one of the high-temperature wells in Iceland.

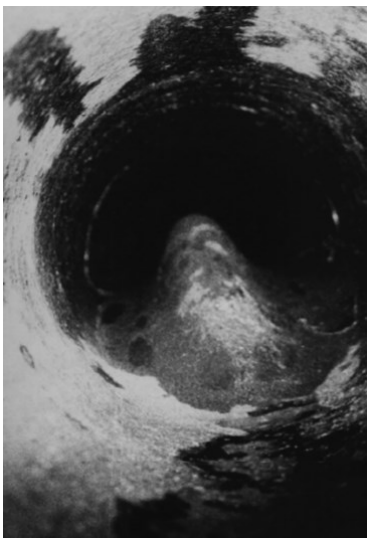

Figure 1: The collapse of a production casing string in a high-temperature well in Iceland due to a potential expansion of entrapped water within the annular cement sheath (Thorhallsson 2003)

It is believed, that even once a high-quality cement coverage, confirmed by cementing reports, hydraulic testing, and cement evaluation log analysis, is achieved, cement sealing ability might be significantly threatened by the rapidly changing temperature and pressure conditions during later stages of well's life cycle (De Andrade et al. 2016) and debonding at casing-to-cement or cement-to-rock interfaces and/or cement cracks might occur.

2. LOS HUMEROS GEOTHERMAL FIELD

The LHGF is one of the four productive geothermal fields in Mexico, located at the border of Veracruz and Puebla states and administrated by the Comisión Federal de Electricidad (CFE). It is a high-enthalpy field with two main distinctive feed zones, one being liquid dominant with hydrostatic pressures, located at depths between 1150 and 1800 m with temperatures ranging between 290°C and 330°C and second, 2-phase to steam-dominant, with near-boiling pressures and temperatures ranging between 300°C and 400°C located at depths between 2100 and 2800 m (García-Gutiérrez et al. 2009). The field consists of approximately 25 production wells with several injection wells and an overall installed capacity amounting to 95.7 MW_e. In recent years, a significant decrease of liquid saturation has been observed due to the insufficient reservoir recharge. A plan to develop unconventional geothermal resources is currently underway in Mexico. One of such initiatives is GEMex[1] (Horizons 2020) project, which aims to increase energy production from the hydrothermal LHGF and not yet developed petrothermal Acoculco field with two deep high-temperature "dry" wells, that proved to be good candidates for the development of the enhanced geothermal system (EGS). Despite a large amount of research concerning the development of the LHGF such as geochemical, geophysical and geological modeling, a broad study on the reservoir geomechanical modeling has not been carried out yet, and geomechanical character of the reservoir is not precisely known.

Table 1: Well construction of the high-temperature "A" well in the LHGF (courtesy of CFE)

Open hole diameter, inch	Casing outer diameter, inch	Casing grade	Casing weight, lb/ft	Casing depth, m
40	30	B	98.93	5
26	20	K-55	54.5	62
17 ½	13 ⅜	K-55	54.5	498
12 ¼	9 ⅝	TN 80–Cr3%	47	1297
8 ½	7 (liner pipe)	TN 80–Cr3%	29	1250 – 1293
8 ½	7 (liner pipe)	TN 80–Cr3%	29	1293 – 2352

The investigation carried out in this paper is based on the results from the high-temperature well "A" (Table 1), located within the central part of the Los Humeros caldera intersecting the inferred Cueva Ahumada fault. The well's kick-off point is located at a depth of approximately 1000 m with a horizontal displacement of 353 m. The final measured depth was 2360 m and true vertical depth 2310 m. The well was drilled from 12 m to 1300 m with water-based bentonitic drilling fluid with a fluid density ranging from 1.01 to 1.06 g/cm^3, whereas an underbalanced method was used in the deeper reservoir well sections.

3. IN-SITU STRESS CONDITION PREDICTIONS

There are number of existing methods for assessing the stress state of the reservoir which include earthquake focal mechanisms, wellbore deformations (i.e. borehole breakouts and drilling-induced fractures), young geologic data (i.e. fault-slip analysis and

[1]http://www.gemex-h2020.eu

volcanic vent alignment) and direct in-situ stress measurements (e.g. overcoring or hydraulic fracturing) (World Stress Map, 2016). Relative estimations of stress regime and their magnitudes might be also carried out using sonic logging, by applying a set of available models and empirical correlations, a method common to the petroleum industry. Obtaining reliable estimations of parameters such as pore pressure (P_p), S_v, S_{hmin}, and S_{Hmax} is vital for ensuring safe operations throughout the lifecycle of a geothermal well. Unfortunately, direct in-situ measurements of crustal stresses, only methods that can provide absolute value of S_{hmin}, are rarely included in the logging campaigns of deep geothermal wells in high enthalpy fields. It is mainly due to technical difficulties resulting from extreme formation temperatures and often heavily fractured formations. The P_p in a geothermal system describes the pressure of the fluid within pores of an underground reservoir and it changes as fluids are being produced. The computation of the P_p is not trivial and is commonly performed by selecting the fixed point of pressure at the pivot point, obtained from pressure logs during well heating up, as representative of local hydraulic head feeding the well.

For investigation carried out in this study and due to the limited amount of data available from the LHGF, two in-direct methods were investigated for relative predictions of in-situ stress magnitudes and their orientations. The first method is based on the localised borehole breakouts (BO) using a six-arm mechanical caliper log and includes predictions of S_{Hmax} orientation from the developed ellipse-fitting method and estimations of magnitude values of S_{hmin} and S_{Hmax} assuming the so-called "stable arch" approach with BO width of 90° (Zoback 2007). The second method allows predicting lower bound on S_{hmin} based on the localized intervals of circulation fluid loss, recomputing the total applied wellbore pressure during drilling.

3.1 Borehole breakouts

BO's, as presented in Figure 2, are spalled symmetrical regions at each side of the borehole wall, centred at the azimuth of the S_{hmin} and located perpendicular to the S_{Hmax}, found in any type of formation rock and tectonic environment in which the average azimuth of the long interval section is consistent within a given field. These enlargements of the borehole wall are caused by the failure that takes place once maximum tangential wellbore stresses exceed the compressive strength of the formation rock (Zoback 1985 and 2007). Such a situation may happen during drilling, once spalled rock is being washed out by the circulating drilling fluid, thus orthogonal spalling appears on the wellbore wall. Laboratory studies carried out by Haimson and Edl (1972) have proven that BO's extend throughout the circumference of the borehole and their depth presents a clear increase in respect to the increase of confining pressure. These claims were later confirmed by Haimson and Herrick (1985), which concluded that the BO width and depth are directly related to the magnitude of the S_{hmin}.

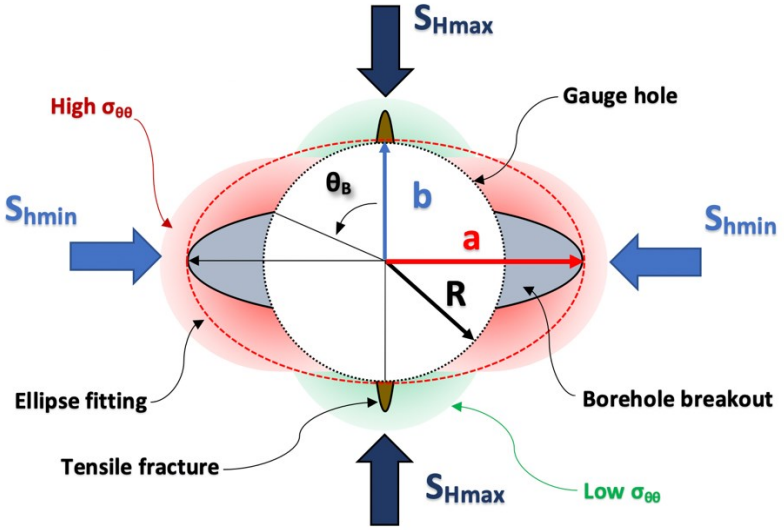

Figure 2: The borehole cross-section with acting horizontal stresses and ellipse fitting approach (a – semi-major axis, b – semi-minor axis, R – in-gauge hole radius, θ_B – an azimuth measured from the direction of S_{Hmax})

3.1.1. Constraining S_{Hmax} orientation

The two possible ways of localizing BO intervals include either mechanical four or six-arm caliper logs, primarily used for estimating cement volumes, and azimuthal image logs. The six-arm caliper tool, in comparison with four-arm, has two additional arms with all them being separated by an interval of 60°. From both tools, the four-arm caliper is more commonly used for stress orientation acquisition (Plumb and Hickman, 1985), due to the only two pairs of caliper pads being centred in the borehole in comparison with the often off-centred six-arm caliper (Zajac and Stock, 1997).

Calculating BO's orientation from six-arm mechanical caliper is not a straight-forward procedure. Wagner et al. (2004) compare four different methods of decentralization correction of six-arm caliper logs in different downhole conditions and concluded that circle-fitting (Baessler, 1995) and centre of mass (Barton, 1988) methods have poor performance in noncircular and result in a center offset in circular holes. They concluded that ellipse-fitting (Lysne, 1986) and chord approach result in best corrections for caliper decentralization, with chord approach providing a large amount of error in big key seats. The main problem with ellipse fitting method found was that at times hyperbola, instead of an ellipse, may be fitted onto the caliper recordings. Zajac and Stock (1997) presented a method of calculating BO orientation from six-arm caliper log assuming the orientation of the longest caliper arm as an elongation direction. It is, however, not said explicitly that the longest arm will track the elongation direction.

As there is no single approach that can be expected to give an optimal correction for decentralized six-arm caliper tool, the ellipse fitting approach (presented in Figure 2) was selected to compute maximum and minimum open hole diameters, borehole centre and BO orientation (assumed here as the orientation of the semi-major axis). The equation used to obtain the best fit from given six-arm mechanical caliper measurements was a general conic equation. The five parameters can be solved from least squares using the measured pad coordinates. It is worth noticing, that the four-arm caliper is not sufficient to fit an ellipse onto caliper points without significant ambiguity. For fitting an ellipse onto the caliper recordings at least five data points are necessary.

3.1.2. Constraining relative magnitudes of S_{hmin} and S_{Hmax}

To calculate the S_{hmin} and S_{Hmax} from the six-arm mechanical caliper log, equations by Kirsch (1898), Jaeger (1961), Zoback (1985) and empirical assumptions by Byerlee (1978) were applied. There a cylindrical hole is considered in a thick, homogeneous, isotropic and elastic plate subjected to a maximum and minimum principal stress. Assumptions made for computations of S_{hmin} and S_{Hmax} and include no excess pressure in the wellbore and S_{Hmax} being smaller or equal to $3S_{hmin}$, which is always the case in situ (Brace and Kohlstedt 1980 and Zoback 2007). Using four- or six-arm caliper tools cannot provide reliable information about the BO width for calculations of stress magnitudes. Such parameter can be only acquired once azimuthal image logs are available. To obtain relative magnitudes of in-situ stresses, an assumption was made that the wellbore is in the equilibrium state, where BO width amounts to 90º. A BO width exceeding 90º amounts to the failure of more than half of the borehole's circumference and as a result well lacks adequate arch support. Inadequate support of the arch leads to the failure all around the borehole.

3.2 Fluid circulation losses

The S_{hmin} value is usually determined using LOT results. Such estimates are often inaccurate due to the possible existence of drilling-induced or natural fractures, unknown stress concentration or variability in the test procedures applied and eventually lead to significant discrepancies between LOT results and actual S_{hmin}. Additionally, LOT's are rarely conducted, especially in high-temperature reservoirs, and oftentimes are not optimised to determine in-situ stress values (Edwards et al. 2002). Measurements of S_{hmin} may, however, be carried out "accidentally" during drilling operations once circulation fluid loss occurs. Drilling fluid circulation losses are the result of the applied total wellbore pressure exceeding the minimum principal stress in the open hole section of the wellbore, leading to its tensile failure. This assumption allows assessing the lower bound on S_{hmin} at intervals of drilling fluid loss, assuming that no pre-existing open fractures were encountered. An assumption was made, that whenever total wellbore pressure applied does not change, i.e. applied pressure becomes insensitive towards the fluid loss, S_{hmin} was exceeded. For longer intervals of drilling fluid loss, averaged total wellbore pressures were assumed as S_{hmin}.

3.3 Results

For the analysis of BO with use of six-arm caliper tool in the "A" well, the vertical section between 496 and 1100 m was selected, as the tool deviation within these depths is less than 10°. The filtration procedure for selecting BO intervals rejects caliper records that do not meet the filtration criteria described by Zajac and Stock (1997). Due to lack of destructive testing of rock samples from the LHGF reservoir, a literature search on basic mechanical and elastic properties of formation rock was carried out. The assumption was made, that studied vertical well section was drilled in homogenous formation rock. The bulk density of the formation rock was assumed as 2540 kg/m^3, elastic modulus as 30 GPa, Poisson's ratio as 0.25, compressive strength as 113 MPa and tensile strength as 12 MPa with an angle of internal friction of 40° (Siratovich et al. 2012 and 2014, Molenda et al. 2013). Results of the two described stress indication methods are presented in Figure 3.

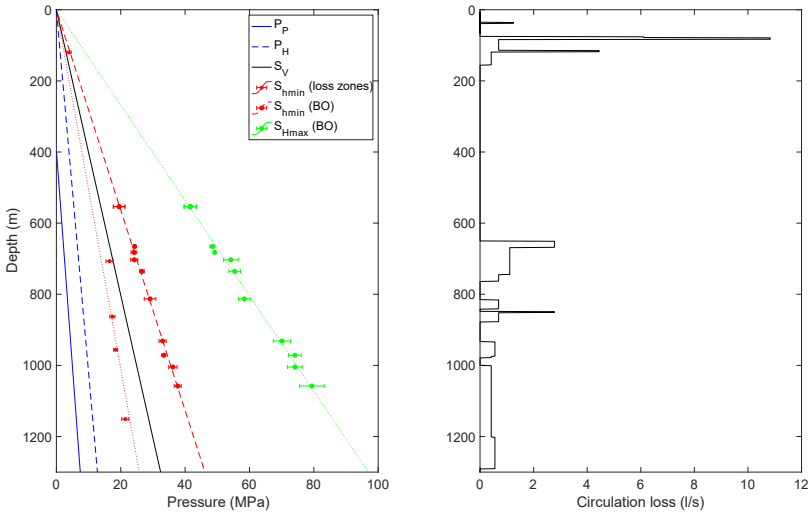

Figure 3: Relative magnitudes of S_{hmin} and S_{Hmax} based on the BO's and circulation fluid losses and registered circulation losses (P_H – hydrostatic pressure) in the "A" high-temperature well

From the deformation analysis in the vertical section between 496 to 1110 m in the "A" well 10 zones of BO's were identified. Results presented in Figure 3 indicate that the well "A" exhibits between strike-slip ($S_{hmin} < S_V < S_{Hmax}$), based on the circulation losses approach, to reverse ($S_v < S_{hmin} < S_{Hmax}$), based on the analysis of BO's, faulting regime. An average orientation of S_{Hmax} amounted to N 94.3° W with a standard deviation of 21°, mean BO interval depth of 812 m and maximum rotation in the range of 42°. The total

length of the identified BO's amounted to 332 m. Accordingly, to the WSM classification from 2016, identified BO's from the "A" well fall into C quality ranking. Resultant calculations of stress magnitudes can be used for the coupled cement sheath failure analysis using the methodology developed by Kruszewski et al. 2019.

4. CEMENT SHEATH INTEGRITY MODEL

The mechanical cement sheath design for long-term performance is a relatively new practise of the petroleum industry (Nelson and Guillot 2006). Such practise has not yet gone mainstream in the geothermal industry where interest in mechanical and elastic parameters of hardened cement other than compressive strength is still rather low and concepts for cement sheath design, considering the role of debonding, cracks and plastic behavior, etc., are still to be evolved. Common wellbore cement design practice assumes that geothermal well cement should exhibit a minimum compressive strength of 6.9 MPa and minimum water permeability of 0.1 mD (API Task Group, 1989). However, recent studies (Philippacopoulos et al. 2002, Teodoriu et al. 2010, Liu et al. 2017), concluded that even at high compressive strengths, cement might not provide proper zonal isolation.

The combined effect of low permeability and tensile strength of the cement matrix leads to serious mechanical damage of the saturated annular cement at temperatures equal to or higher than the boiling point of water at depth. Increased porosity of annular cement sheath, often created due to the poorly executed cementing job, results in deterioration of its mechanical and elastic properties, which play an important role especially after the execution of the primary cementing job. The study on how the mechanical, elastic and thermal properties of the casing-cement-rock system, its geometry, acting in-situ stresses, applied wellbore pressures, and temperature conditions influence the cement sheath stresses is important not only for the proper selection of the cement slurry but also for the definition of allowable pressures and temperatures during the well's life cycle and prediction of cement sheath failure.

4.1 Cement sheath failure

Failure of wellbore cement sheath might be related either to its structure or material. Structural failure includes cement debonding, i.e. so-called microannulus, at either casing-to-cement or cement-to-rock interface achieved due to high thermo-mechanical post-cementing stresses exerted on the annular cement sheath during operations such as stimulation, injection, hydraulic fracturing, fluid production kick-off or well quenching, exceeding material resistance (Wehling 2008). Material mechanical failure manifests itself as chimneys or channels propagating within the bulk of cement (Loizzo 2014). Such failure is usually created once the cement is in a liquid state or during the curing phase, which usually from 3 to 5 days. The main reason for such defects is the faulty execution of drilling operations and/or primary cementing job (Teodoriu et al. 2013). Material failure also includes tensile and shear cracks within the bulk of cement sheath, similarly to debonding scenario, due to high thermo-mechanical stresses created during various well operations after the cement slurry is hardened.

4.2 Annular cement performance analysis

Sonic and ultrasonic acoustic logging tools are commonly used in the drilling industry to evaluate the quality of annular cement and the degree of bonding at the casing-to-cement interface. Throughout the years, the main procedure was to correlate the attenuation rate of an extensional wave propagating at a sonic frequency with the cement compressive strength values (Pardue et al. 1963). A study carried out by Jutten et al. in 1989, based on numerous laboratory experiments, proved that it is not the compressive strength but the acoustic impedance that exhibits high correlation with attenuation rate, regardless of cement type. This led to the development of improved interpretation correlating attenuation rate, acoustic impedance, and cement's compressive strength. With a joint interpretation of sonic and ultrasonic measurements, a much clearer picture of cement performance is obtained, allowing for better cement quality evaluation and potential detection of microannulus (Nelson and Guillot 2006). Results from a comparative analysis of both sonic and ultrasonic logs from the "A" well is presented in Figure 4.

Microannulus, i.e. deboning at casing-to-cement or cement-to-rock interface, is regarded as a small liquid (wet microannulus) or gas (dry microannulus) filled gap, usually with less than a few hundred micrometers in thickness, created due to pressure and/or temperature changes in the wellbore (Nelson and Guillot 2006) or faulty cementing job. The presence of microannulus implies that bonding at the interface is lost and in effect, wellbore integrity is threatened. Dry microannuli are created either by formation gas intrusions or by excessive thermo-mechanical stress resulting from changes in temperature or pressure, whereas water-filled ones are created by the intrusion of reservoir fluids. The dry microannuli are believed to be thinner than water-filled ones. In water-bearing systems with high fluid circulation, like most of the productive hydrothermal reservoirs, it is more believed that wet microannuli will be encountered. It is however not necessarily uncommon, to encounter dry microannuli in such conditions, which imply unconnected annular cement defects.

The fluid-filled microannulus at the casing-to-cement interface, was observed in the case study of the "A" well (Figure 4). This can be evidenced by the low values of sonic acoustic impedance recordings, that 'see' liquid in most sections concerining the ultrasonic acoustic impedance, which in most parts of the 500 m interval 'sees' low to medium impedance cement and medium to high impedance cement in the last 150 m section. Therefore, there might be a sizeable liquid layer, which may expand and potentially boil threatening wellbore integrity. The key question is whether such layer is isolated or not. Isolated liquid pockets, as mentioned before, will flash and collapse the production casing. It is, however, believed that debonding fractures are connected and pressure might be self-regulated either at the source (i.e. aquifer) or at the surface.

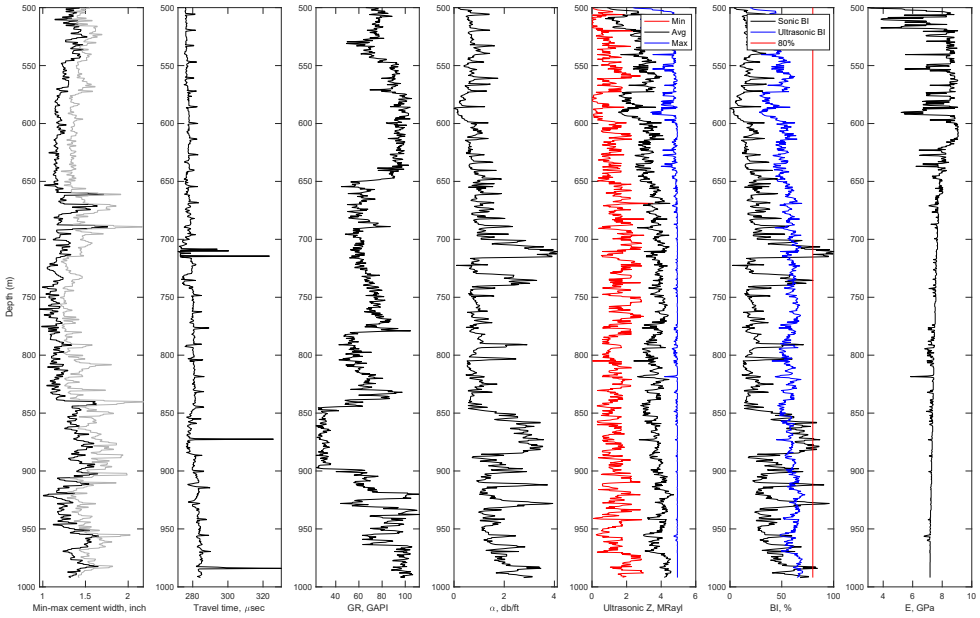

Figure 4: Wire-line logging results of the cement sheath behind the production casing in the 500 m vertical section of the high-temperature geothermal well "A"

The low-impedance pixels on the azimuthal impedance map are significantly affected by debonding, and not by the weaker annular cement behind the steel casing. Therefore, once the presence of microannulus, based on comparative analysis of sonic and ultrasonic logs, is verified one cannot utilize average values of acoustic impedance for recalculating mechanical and elastic properties of annular cement. Such properties are determined primarily by bonding conditions and minimum or average ultrasonic acoustic impedance measurements are therefore not reliable. To carry out computations of cement properties, maximum values of ultrasonic acoustic impedance, less affected by debonding, recalculated from the azimuthal impedance map should be utilized. Example of such digitalized azimuthal impedance map for the interval between 12.5 and 82.5 m from the "A" well within the LHGF is presented in Figure 5.

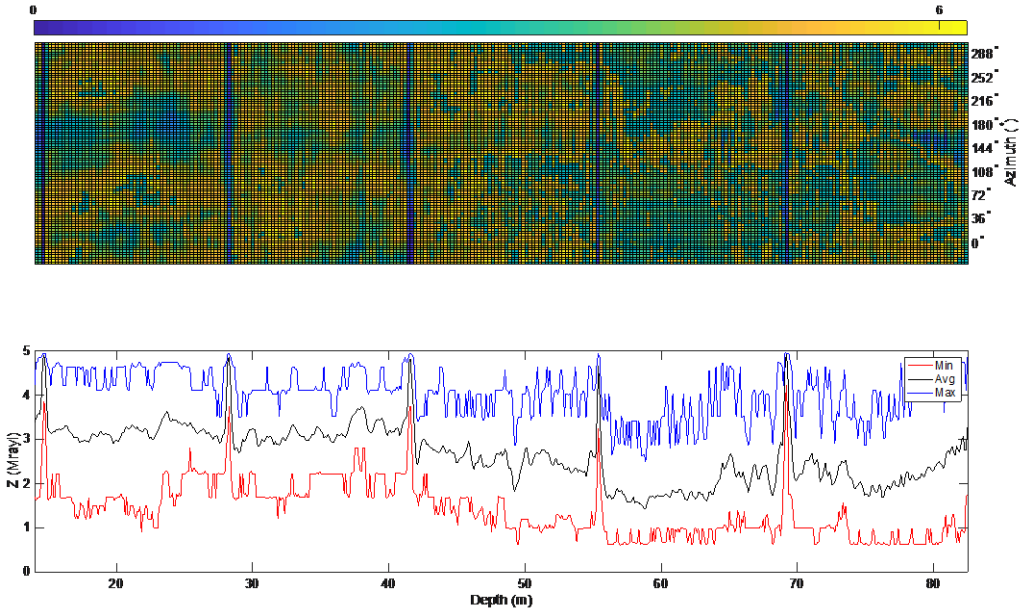

Figure 5: Calculation example of minimum, average and maximum values of ultrasonic acoustic impedance (bottom) based on the pixelized azimuthal impedance map from the ultrasonic bond log (top) at shallower depths of the "A" well

To analyze the annular behavior of cement and infer mechanical parameters of annular cement workflow model based on correlations developed by Pardue et al. (1963), Jutten et al. (1989 and 1993) and Kalyanraman et al. (2017) was established. It is worth mentioning, that properties of cement as well as bonding at interfaces are not constant and change throughout well life cycle in comparison to

rock properties which stay unchanged. Therefore, sonic and ultrasonic logs are only a representation of hardened cement at a particular time. In this case study, it is 120 hours after cement placement.

4.3 Analytical model

To calculate potential cement failure, the stress state within the wellbore cement sheath has to be assessed. To do so, the analytical axisymmetric model by Ugwu (2008) and Teodoriu (2010), treating the casing-cement-rock as a multi-cylinder setup, was selected. The model, that assumes casing as a thin-walled cylinder and both cement and formation rock as thick wall cylinders, accounts for:

- mechanical properties of the coupled casing-cement-rock system,
- isotropic in-situ stresses,
- applied wellbore pressures,
- temperature effect (temperature difference between the fluid inside the casing and formation temperature).

It is widely known, that in-situ stresses are mainly anisotropic, however, the approximation of isotropic in-situ stresses, as made in this particular analytical model, is enough to address weaknesses in the annular cement. The casing-cement-rock coupled system is regarded as a pressurized composite system, without initial stresses existing in cement, with three concentric cylinders and a perfect bonding at casing-to-cement and cement-to-rock interfaces. The casing-cement-rock composite cylinder undergoes plane strain deformation (Ugwu 2008). The model assumes a casing inner diameter of 8.681" and an outer diameter of 9.625" with a wall thickness of 0.472". An inner diameter of cement sheath is equal to the outer diameter of a casing string, whereas the outer diameter of cement sheath, which is simultaneously the inner diameter of rock formations, was assumed as an average value of the minimum and maximum open hole diameter measured using caliper. The outer diameter of formation rock assumed as 20". The elastic modulus of the 9-5/8" production casing material, with a nominal weight of 47 lb/ft and TN 80-Cr3% steel grade was de-rated for the maximum internal wellbore temperature to which steel was exposed to during various well operations using NZS2403:2015. Poisson's ratio of casing steel was de-rated for temperature using correlations by Ancaş (2006), whereas the coefficient of thermal expansion was de-rated for temperature using correlation by Chevron Corporation (2005). Cement used for primary cementation job of 9-5/8" production casing in this case study was class H cement with a density of 1800 kg/m^3 and 40% BWOC of silica flour, to prevent strength retrogression (Eilers et al. 1983). The angle of internal friction of cement between 20° (Ochepo et al. 2012) and 57.5° (Fujita et al. 1998) was assumed for the prediction of cement sheath shear failure.

4.4 Results

Different loading scenarios, imitating the life cycle (e.g. drilling, production and maintenance operations) of the high-temperature geothermal well may be investigated for a proper wellbore cement design in terms of pressure management. In this study, an undesirable event of well quenching (i.e. killing of the well with cold water) where internal pressure exerted upon a production casing string is close to the hydrostatic water column with an assumed temperature of killing fluid (i.e. water) of 100°C was studied and presented in Figure 6. Temperature and pressure profiles, together with pore and fracture pressures, used for cement sheath stress predictions, were taken directly from results of the logging campaigns. Additional loading scenarios for high-temperature wells, that were not investigated in this particular study, might include production kick-off with use of gas-lift, long time fluid production, hydraulic fracturing or acidification. Compressive stresses are presented in the figures as negative, whereas tensile as positive values.

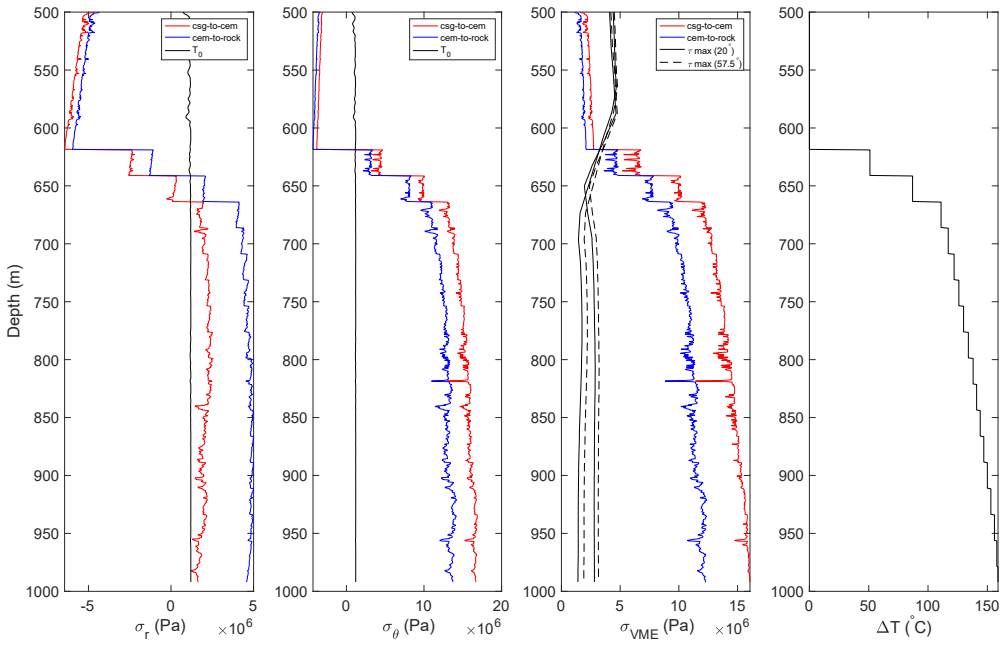

Figure 6: Radial, tangential, and VME stresses in the cement sheath during well quenching operations (values were smoothed for better data visualization)

For the maintenance loading scenario of well quenching, hardened cement prevails undamaged in an interval between 500 and 625 m. Below this depth, all stresses become tensile and greatly exceed the tensile strength of annular cement leading to its failure in tensile as well as in shear mode. In this loading case, the main factor controlling the potential cement failure is the temperature difference between colder quenching fluid and hotter adjacent rock formations.

1. CONCLUSIONS

- The "A" well exhibits between strike-slip ($S_{hmin} < S_V < S_{Hmax}$) and reverse ($S_v < S_{hmin} < S_{Hmax}$) faulting regime based on the two investigated methods for an indication of in-situ stress conditions. An average orientation of S_{Hmax} amounted to N 94.3° W with a standard deviation of 21°.
- Primary cementing of high-temperature geothermal wells is a fundamental procedure that has to be executed properly and supported by detailed stress analysis under expected pressure and temperature conditions throughout different stages of a well life cycle.
- For a properly designed wellbore cement in terms of general pressure management, any possibilities of abrupt temperature changes between well and surrounding rock formations shall be excluded.
- To prevent pre-mature cement failure, it is advised to improve the elastic properties of the hardened cement slurry. This can be carried out by adding plasticizers to the cement mixture, lowering cement slurry density or by replacing conventional cement slurries with non-Portland sealing systems.

ACKNOWLEDGMENTS

Authors would like to thank CFE in Morelia and Los Humeros for providing the data for this publication as well as for constructive criticism during the preparation of this paper. GEMex has received funding from the European Union's Horizon 2020 research and innovation program under grant agreement No. 727550.

REFERENCES

Ancaş, A. and Gorbănescu, D.: Theoretical models in the study of temperature effect on steel mechanical properties, *The Bulletin of the Polytechnic Institute of Jassy*, (2006).

API Task Group on Cements for Geothermal Wells: API Work Group Reports Field Tests of Geothermal Cements, *Oil and Gas Journal*, Pages 93-97 (1985).

Baessler H.: Dezentrierungskorrektur von BHTV-Daten angewandt auf die Tiefbohrung VGS-Russland und Hochaufloesende Kaliberauswertung am Beispiel der KTB, Geophysical Institute, University of Karlsruhe, *Diploma Thesis* (1995).

Barton, C.: Development of in-situ stress measurement techniques for deep drill holes, *Dissertation*, Stanford University, USA (1988).

Brace, A.B. and Kohlstedt D.L.: Limits on lithospheric stress imposed by laboratory experiments, *Journal of Geophysical Research*, 85, 6248-6252 (1980).

Byerlee, J.: Friction of Rocks, *Pageoph*, Vol. 116, Birkhfiuser Verlag, Basel (1978).

Chevron Corporation: Casing/Tubing Design Manual, San Ramon, California, U.S. (2005).

Edwards, S. T., Bratton, T. R., Standifird, W. B.: Accidental Geomechanics – Capturing In-situ Stresses from Mud Losses Encountered while Drilling, SPE/ISRM 78205, Presented at the SPE/ISRM Rock Mechanics Conference in Irving, Texas (2002).

Fujita, Y., Ishimaru, R., Hanai, S., Suenaga, Y.: Study on Internal Friction Angle and Tensile Strength of Plain Concrete, *Fracture Mechanics of Concrete Structures Proceedings FRAMCOS-3* (1998).

García-Gutiérrez, A.: Estado térmico inicial del campo geotérmico de Los Humeros, Puebla, *Geotermia*, Vol. 22, No. 1, pp. 59-69 (2009).

Haimson, B.C. and Edl, J.N.: Hydraulic fracturing of deep wells, SPE Paper No. SPE 4061, (1972).

Haimson, B.C. and Herrick, C.: In-situ stress evaluation from borehole breakouts: experimental studies, in *Proc. 26th US Symp. Rock Mech.*, Rapid City, Balkema, Rotterdam, 1207-1218 (1985).

Heidbach, O., Rajabi, M., Reiter, K., Ziegler, M., WSM Team: World Stress Map Database Release 2016, V. 1.1. GFZ Data Services (2016).

Jaeger, J. C.: Elasticity, Fracture and Flow, 212 pp., Methuen, London (1961).

Jutten, J.J., Guillot, D., Pareevaux, P.A.: Relationship Between Cement Slurry Composition, Mechanical Properties, and Cement-Bond-Log Output, SPE-16652-PA, *SPE Production Engineering* (1989).

Kalyanraman, R.S., Van Kuijk, R., Hori, H.: Making Sense of Why Sometimes Logs Do Not See Cement in the Annulus, *SPE Western Regional Meeting*, 23-27 April, Bakersfield, California, SPE-185731-MS (2017).

Kirsch, G.: Die Theorie der Elastizitat und die Beaurforisse der Festigkeitslehre, V DI Z 1857 1968, 42, 707 (1898).

Kruszewski M. and Wittig V.: Review of failure modes in supercritical geothermal drilling projects, *Geothermal Energy, Science – Society – Technology*, 6:28 (2018).

Kruszewski, M., Montegrossi, G., Ramirez Montez, M., Wittig, V., Gomez Garcia, A., Sanchez Luviano, M., Bracke, R.: A wellbore cement sheath damage prediction model with the integration of acoustic wellbore measurements, *Geothermics*, Volume 80, Pages 195-207 (2019).

Liu, W., Yu, B., Deng, J.: Analytical method for evaluating stress field in casing-cement- formation system of oil/gas wells, *Applied Mathematics and Mechanics*, Volume 38, Issue 9, Pages 1273–1294 (2017).

Loizzo, M.: Long-term well integrity: Geothermal energy and annular leak prevention, *Conference proceedings from 5th VDI-Fachtagung Geothermische Technologien*, Hannover, Germany (2014).

Lysne, P.: Determination of borehole shape by inversion of televiewer data, *The Log Analyst*, vol. 27, no. 3, p. 64 – 71 (1986).

Molenda, M., Stöckhert, F., Brenne, S., Alber, M.: Comparison of Hydraulic and Conventional Tensile Strength Tests, Effective and Sustainable Hydraulic Fracturing Rob Jeffrey, IntechOpen (2013).

Nelson, B.E. and Guillot, D.: Well Cementing, 2nd Edition, *Schlumberger* (2006).

Ochepo, J., Stephen, O.D., Masbeye, O.: Effect of Water Cement Ratio on Cohesion and Friction Angle of Expansive Black Clay of Gombe State, Nigeria, Department of Civil Engineering, Vol. 17 (2012).

Pardue, G.H. and Morris, R.L.: Cement Bond Log-A Study of Cement and Casing Variables, SPE-453-PA, *Journal of Petroleum Technology*, Vol. 15, Issue 5 (1963).

Philippacopoulos, J.A. and Berndt, L.M.: Structural analysis of geothermal well cements, *Geothermics*, Volume 31, Issue 6, Pages 657-676 (2002)

Plumb, R. A. and Hickman, S.H., Stress-induced borehole elongation: a comparison between the four-arm dipmeter and the borehole televiewer in the Auburn geothermal well, *Journal of Geophysical Research*, vol. 90, no. B7, p. 5513 – 5521 (1985).

Robertson, E.C.: Thermal properties of rocks, *U.S. Geological Survey open-file report*; Pages 88-441, US Geological Survey (1988).

Siratovich, A.P., Davidson, J., Villeneuve, M., Gravley, D., Kennedy, B., Cole, J., Wyering, L., Price, L.: Physical and Mechanical Properties of The Rotokawa Andesite from Production Wells Rk 27_L2, Rk 28 And Rk 30, *New Zealand Geothermal Workshop 2012*, Auckland, New Zealand (2012).

Siratovich, P.A., Heap, M.J., Villenueve, M.C., Cole, J.W., Reuschlé, T.: Physical property relationships of the Rotokawa Andesite, a significant geothermal reservoir rock in the Taupo Volcanic Zone, New Zealand, *Geothermal Energy* (2014).

Teodoriu, C., Kosinowski, C., Amani, M., Schubert, J., Shadravan, A.: Wellbore Integrity and Cement Failure at HPHT Conditions, *International Journal of Engineering and Applied Sciences*, Vol. 2, No.2 (2013).

Teodoriu, C., Ugwu, I., Schubert, J.: Estimation of Casing-Cement-Formation Interaction using a new Analytical Model, SPE 131335, *SPE EUROPEC/EAGE Annual Conference and Exhibition held in Barcelona*, Spain (2010).

Thorhallsson, S.: Geothermal Well Operation and Maintenance, Geothermal Training Programme, *IGC2003 - Short Course* (2003).

Ugwu. O.I.: Cement Fatigue and HPHT Well Integrity with Application to Life of Well Prediction, *Master Thesis*, Texas A&M University (2008).

Wagner, D., Mueller, B., Tingay, M.: Correcting for Tool Decentralization of Oriented Six-Arm Caliper Logs for Determination of Contemporary Tectonic Stress Orientation, *Petrophysics*, Technical Note, vol. 45, No. 6, p. 530 – 539 (2004).

Wehling, P.: Wellbore Cement Integrity Testing, *Master Thesis*, TU-Clausthal, (2008).

Zajac, B. J. and Stock, J. M.: Using borehole breakouts to constrain the complete stress tensor: Results from the Siljan Deep Drilling Project and offshore Santa Maria Basin, California, *Journal of Geophysical Research*, vol. 102, no. B5, p. 10083 – 10100 (1997).

Zoback, M.D., Moos, D., Mastin, L., Anderson, R.: Well Bore Breakouts and in Situ Stress, *Journal of Geophysical Research*, Vol. 90, No. B7, Pages 5523-5530 (1985).

Zoback, M.D.: Reservoir Geomechanics, Cambridge University Press (2007).